URSI - RCRS 2022, IIT (Indore), India, 1 - 4 December, 2022

Lunar ionosphere in the wake region : evidence for an enhanced plasma density using measurements from DFRS onboard Chandrayaan-2

Keshav R. Tripathi[(1)], R.K. Choudhary [(1)], Ambili KM[(1)], K.R. Bindu[(2)], R. Manikantan [(3)], Umang Parikh[(3)]
(1) Space Physics Laboratory (SPL), VSSC, Trivandrum, Kerala 695021, India
(2) UR Rao Space Centre (URSC), Bangalore, Karnataka 560017, India
(3) ISRO Telemetry, Tracking, and Command Network (ISTRAC), Bangalore, Karnataka 560058, India

Abstract

The DFRS (Dual Frequency Radio Science) payload onboard the Chandrayaan-2 orbiter is conducting radio occultation (RO) experiments using coherent X-band and S-band radio signals in one-way dual-frequency RO mode. We present 'first of its kind measurements of the enhanced integrated electron density (along the path) profiles (iEDPs) in the lunar wake and trans-terminator regions. Detailed analysis of the results shows that the integrated electron content of the lunar ionosphere can be as large as ∼1.5 TECU, (1 TECU = 10^{16} m^{-2}) in the lunar wake region. Large electron content is also seen near lunar polar regions during solar transition periods. These observations are unique in nature as they show post-sunset enhancements in the iEDPs compared to dayside, as reported by earlier missions. These findings further support the theory for the formation and sustenance of the lunar ionosphere as suggested by 3D lunar ionospheric modeling effort by [1].

1. Introduction

The Moon, Earth's natural satellite, is a planetary body whose surface is covered with regolith, possesses a tenuous surface-bound exosphere (SBE), and is devoid of a global intrinsic magnetic field [3]. The SBE is populated by out gassing from the lunar regolith by high energetic processes [8], including hypervelocity micrometeoric impact solar wind, and uplift of charged lunar dust by the surface electric field produced by solar photon [3]. The photoionization of this tenuous atmosphere by solar EUV and X-rays radiations forms a detectable lunar ionosphere [4]. Apart from this classical way of production of the ionosphere, the processes such as solar wind sputtering and micrometeorite impact, also produce charged particles along with the neutrals. The charge exchange reactions of solar wind protons and electrons with the ambient neutrals from another source form the detectable presence of lunar ionosphere at nightside [1].

The first observation of the lunar ionosphere was made by Luna 19 and Luna 22 spacecraft, both observed peak electron density, ∼1000 cm^{-3} , near to the surface in the dayside trans-terminator region [9]. Japan's recent moon mission, the second lunar mission SELenological and ENgineering Explorer (SELENE), had several sophisticated experiments onboard to probe the lunar ambiance. In addition, two mini spacecraft (V-star and R-star) were also employed to probe the tenous lunar ionosphere. They were used so as to avoid the effect of interplanetary medium and/or terrestrial atmosphere on the radio signals in radio science experiments [2]. Measurements using the combination of two mini-satellites observed the vertical electron density profiles mostly for solar zenith angle (SZA) to be less than 60°. Observed electron density peak was about 350 cm^{-3}, close to the surface with the integrated total electron content (TEC) of the order of 0.06 TECU. Here, 1 TECU (or 1 hexem) is equal to 10^{16} m^{-2}. A similar result was later reported by Chandrayaan-1 measurements as well [4].

In a recent work [1], the three dimensional distribution of lunar ionospheric electrons and ions produced by the photochemical reactions, showed that the surface electron density at the Moon, at times, could be as high as 1.2 × 10^5 cm^{-3} over the mid-latitudes, if dynamical interaction between the solar wind and lunar plasma is not accounted. The absence of any intrinsic magnetic field, ho we ver, leads the ionosphere on the Moon to interact continuously with the solar wind and results in the removal of ions/electrons. Such interactions, as a result, produce an ionosphere with a maximum electron density ∼1600 cm^{-3} in the lunar polar regions. Another interesting finding was that though the source of photoionization was not available during the midnight/post-midnight periods, the charge exchange reactions with solar wind electrons and protons helped to maintain a 'dense' ionosphere even at the midnight and post-midnight periods at all the latitudes, with the maximum centered around the mid-latitude region. This suggests that photochemistry has strong control over the net electron density distribution in the lunar ionosphere, though solar wind acts as a strong removal agent. Therefore, in a region where the solar wind interaction with the lunar plasma is not important (like in the lunar wake region), a comparatively higher plasma density can be expected. The similar result is observed by DFRS measurements.

2. DFRS Experiments

DFRS payload onboard Chandrayaan-2 spacecraft comprises an evacuated miniaturized crystal oscillator (EMXO) generating two coherent radio signals at S (2240 MHz), and X (8496 MHz) bands of radio frequencies. Technical details and configuration of the payload are given elsewhere [5]. A total of 12 radio occultation experiments have been conducted so far in campaign mode on four different occasions. Those occasions were selected depending upon suitable geometry for the RO measurements and feasibility with other onboard payloads. A list of successful experiments is given in Table (1). Due to spacecraft mounting constraints, simultaneous reception of both X and S-band signals close to egress is difficult, hence only ingress measurements are analysed in this paper. Also, the experiments which do not have residuals up to 90 km altitude are discarded for baseline fitting.

Table-1 Radio occultation events

Date	Orbit#	SZA*	Latitude	SEM*	Std*.
04-10-2019	0489	95^0	-86^0	75^0	0.079
01-02-2020	1958	133^0	47^0	83^0	0.308
01-02-2020	1960	130^0	50^0	84^0	0.158
19-08-2021	8848	84^0	-83^0	143^0	0.090
28-09-2021	9937	89^0	86^0	92^0	0.098
29-09-2021	9939	90^0	85^0	91^0	0.082

SZA: solar zenith angle , SEM: angle between sun earth and moon . Std.: standard deviation in observed iEDPs above 40 km altitude. Here iEDPs are the integrated electron density along the ray-path inside Lunar ionosphere.

3. Results

First we have simulated the Earth's magnetosphere and located the position of the moon with respect to the geo-magnetic tail. It was found that in during the experiments, the moon was outside the influence of the Earth's magnetic field. Based on the observations, experiments can be grouped into two parts, namely (a) near trans-terimnator, and (b) inside the lunar wake region.

3.1 Observations in the lunar wake region

Fig.1 (lower panel) shows the retrieved integrated electron density along the path of radio signals while passing through the wake region of the lunar ionosphere. Here, the region with SZA above 95^0 is considered as the wake region. The SZA and latitude information is for 20 km altitude of the occultation point (closest point on radio signal with the lunar surface) and given in Table (1). As shown in the figure, the integrated electron density is maximum near the surface and decreases with altitude. A similar pattern in the integrated electron density was previously reported for dayside [7]. The integrated electron density obtained for the wake region (nightside), however, is relatively high compared to the values observed during the dayside by [7]. A possible reason for such a difference in the magnitude of the iEDPs can be understood from a related work by [1]. They have shown that the Moon can have a higher electron density during night-time, if the charge exchange reactions of solar wind electrons and protons with ambient neutrals are accounted for. In fact, measurements with the SARA experiment onboard Chandrayaan-1 have shown the presence of solar wind protons and electrons in the lunar wake regions when the IMF Bz is weak [6]. During the period when DFRS was operated, the IMF Bz was weak ($\leq\sim 5$ nT, in all three cases), and hence, the presence of solar wind protons and electrons is expected.

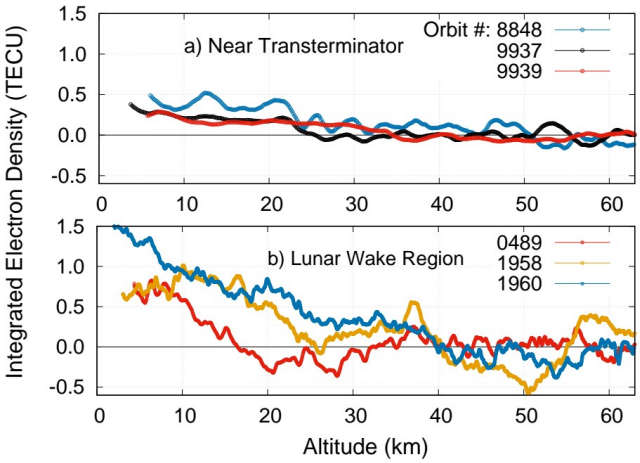

Figure-1 Observed iEDPs in transterminator and polar regions (upper panel) and the lunar wake region (lower panel). The radius of the Moon is approximated as 1736 km. Uncertainty in the observed iEDPs is given in the last column of the Table (1).

3.2 Observations in the lunar wake region

Fig. 2 (upper panel) shows the retrieved iEDPs near the transterminator region of the polar ionosphere at the Moon. These profiles correspond to SZA $\sim 90^0$. Further details are given in Table (1). It is clear from the figure that the iEDP values are relatively less than for the lunar wake region (Fig. 2). But these are still relatively high compared to the values reported [7]. Since these observed profiles are near the polar region, a higher ion concentration than the compared low-latitude regions isexpected [1]. Obviously, a relatively higher density than reported is along the expected line as all the profiles were for the SZA below 60^0. For orbit number 8848, occultation happened at a location near the lunar south pole at a relatively lower SZA, compared to the other observations in the same section of Table (1). This

enhancement in electron density is interesting, and the reason behind this enhancement is subject to further investigation.

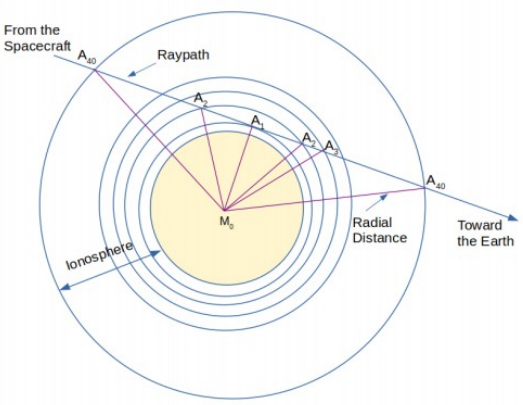

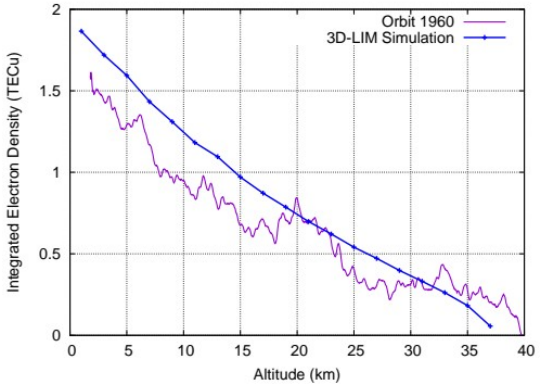

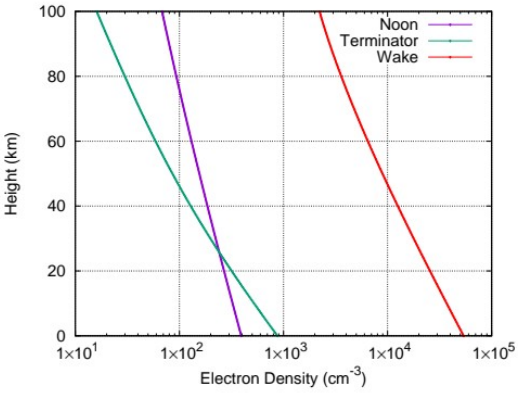

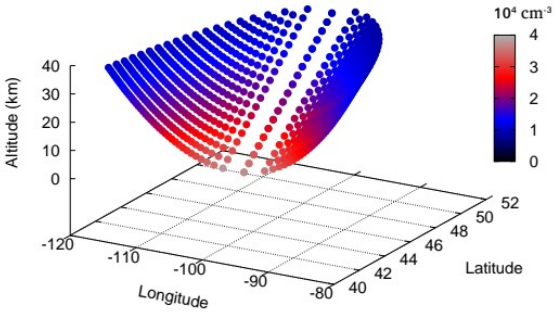

Figure-2 Top left panel: Ray-tracing of radio signals in the lunar ionosphere. A1 is the point of impact factor on the given ray path, **Top right panel**:Comparison of observed and simulated ray-path integrated electron density for the Chandrayaan-2 orbit no. 1960 for the occultation experiment at a location inside the Lunar wake, **Bottom left panel**: Electron density profiles simulated using the 3D-LIM model for three different conditions (Lunar wake, Solar terminator, and local noon). The electron density is of an order of magnitude higher inside the lunar wake region, **Bottom right panel**: Altitude/latitude/longitude variations of electron density along the ray path as simulated by 3D-LIM. The color bar represents the electron density at different points along the radio path. The scale in the color bar is ($\times 10^4$ cm^{-3}). Bottom right-hand panel: comparison of simulated iEDP with observed ones for the orbit no. 1960 for the occultation at a location inside the lunar wake.

3.3 3D-LIM simulations for iEDPs in the lunar wake region

As discussed earlier, using 3D-LIM (three-dimensional lunar ionospheric model) simulations, [1] have shown that the Moon can have an electron density of the order of 1.2 $\times$ 10^5 cm^{-3}, when the interaction of solar wind with the lunar plasma is absent. The maximum electron density is observed at the mid-latitudes with Ar + and Ne + as the major ions which have a comparatively longer lifetime than the molecular ions (CO_2^+ , and H_2O^+), which are dominant ions at other locations. In the top-right panel of Fig. (3), we present 3D-LIM simulated electron density profiles for the Moon under three different conditions, namely when a location is (a) inside the lunar wake, (b) at the solar terminator, and (c) at the local noon. These profiles were simulated for the geosolar conditions as for orbit no. 1960 of Chandrayaan-2. We may note that the surface electron density at the Moon could be of the order of 6 $\times$ 10^4 cm^{-3} , which is two order of magnitude more than at the equator (noon) or near the solar terminator. Here, it is assumed that the solar wind has no influence on the wake region. The top left-hand panel of Fig. (2) shows a schematic ray tracing diagram of a signal transmitted from the spacecraft toward the receiver at the ground station and passing very close to the surface of the moon ($\sim$1738 km from the center of the moon). Consider a plane that contains the ray path, and the Moon, and divide the lunar atmosphere into concentric circular shells with an increasing radius by 1 km in the given plane. The gi ven ray path would intersect concentric circles at different points, i.e. at different altitudes, longitudes, latitudes, and SZAs in the mooncentric coordinate system, shown in the bottom left-hand panel of the figure. Electron density corresponding to these points, simulated by the 3D-LIM model, is represented by colour dots in the figure. The integrated electron density (IED) corresponding to this ray path is $\sim$1.87 TECU. It may be mentioned that the actual path-length of radio signals traversing through the plasma medium could be as high as 700 km, even when the lunar ionosphere is assumed to be limited to 40 km altitude only. Likewise, we simulated all the ray paths at 2 km varying altitude (closest approach) up to 40 km, and estimated the IED. The comparison between simulated iEDP and observed iEDP for orbit number 1960 is shown in the bottom right-hand panel of Fig. (2). We may note that the simulated iEDPs compare quite well with observations. Further details about ray-tracing are given

in the supplementary section. The density profiles corresponding to other conditions shown in the top right-hand panel of the figure also explain why the iEDPs seen by SELENE [2,7] were of an order of magnitude or less than as shown in Fig. (1).

4 Summary and Conclusion

Measurements with the DFRS payload onboard Chandrayaan-2 orbiter are being carried using coherent X -band and S -band radio signals in one way dual-frequency RO mode. Geometrical and/or spacecraft mounting constraints limited the number of occultation events that can be observed, and therefore, our analysis here is limited to the experiments conducted in campaign modes. These profiles are the first of their kind revealing the nature of the ionosphere in the lunar wake region and show that the electron density enhances therein compared to the dayside. The results also show large electron density near the lunar polar regions during the solar transition period. These findings are very much in agreement with a recent simulation study on the lunar ionosphere using a three-dimensional photochemical model [1]. The observ ations, however, are not sufficient enough to discuss either the characteristics or the temporal evolution of the lunar ionosphere. Also, since the observed integrated TEC values are very close to the fluctuations in the TEC of the underlying terrestrial ionosphere, some elements of uncertainties in the derived profiles always stay. These results are very sensitive and need large statistics for broader picture.

Acknowledgements

The DFRS payload was developed at URSC, Bangalore. Special thanks to Kumar Harshit and Rahul K for their help during payload development. Sincere thanks also to all the members of the IDSN-18 and IDSN-32 ground station team; CH2 S/C operation team, specially Debashish Paul and Leo Jackson John; Flight Dynamics team, P/L planning team, Mission Director Ritu Karidhal, and data center teams for their proactive support to conduct RO experiments with DFRS. A special thanks to Himanshu P ande y and P. Gunasekhar of ISSDC for their kind help in data dissemination.

7. References

1. Ambili, K.M. and Choudhary, R.K., 2022. Three-dimensional distribution of ions and electrons in the lunar ionosphere originated from the photochemical reactions. Monthly Notices of the Royal Astronomical Society, 510(3), pp.3291-3300.

2. Ando, H., Imamura, T., Nabatov, A., Futaana, Y., Iwata, T., Hanada, H., Matsumoto, K., Mochizuki, N., Kono, Y., Noda, H. and Liu, Q., 2012. Dual-spacecraft radio occultation measurement of the electron density near the lunar surface by the SELENE mission. Journal of Geophysical Research: Space Physics, 117(A8).

3. Bhardwaj, A., Dhanya, M.B., Alok, A., Barabash, S., Wieser, M., Futaana, Y., Wurz, P., Vorburger, A., Holmström, M., Lue, C. and Harada, Y., 2015. A new view on the solar wind interaction with the Moon. Geoscience Letters, 2(1), pp.1-15..

4. Choudhary, R.K., Ambili, K.M., Choudhury, S., Dhanya, M.B. and Bhardwaj, A., 2016. On the origin of the ionosphere at the Moon using results from Chandrayaan-1 S band radio occultation experiment and a photochemical model. Geophysical Research Letters, 43(19), pp.10-025.

5. Choudhary, R.K., Bindu, K.R., Harshit, K., Karkara, R., Ambili, K.M., Pant, T.K., Shenoy, D., Kumar, C., Reddy, N., Rajendran, T.K. and Nazer, M., 2020. Dual Frequency Radio Science experiment onboard Chandrayaan-2: a radio occultation technique to study temporal and spatial variations in the surface-bound ionosphere of the Moon. Current Science (00113891), 118(2).

6. Dhanya, M.B., Bhardwaj, A., Futaana, Y., Fatemi, S., Holmström, M., Barabash, S., Wieser, M., Wurz, P., Alok, A. and Thampi, R.S., 2013. Proton entry into the near-lunar plasma wake for magnetic field aligned flow. Geophysical Research Letters, 40(12), pp.2913-2917.

7. Imamura, T., Nabatov, A., Mochizuki, N., Iwata, T., Hanada, H., Matsumoto, K., Noda, H., Kono, Y., Liu, Q., Futaana, Y. and Ando, H., 2012. Radio occultation measurement of the electron density near the lunar surface using a subsatellite on the SELENE mission. Journal of Geophysical Research: Space Physics, 117(A6).

8. Stern, S.A., 1999. The lunar atmosphere: History, status, current problems, and context. Reviews of Geophysics, 37(4), pp.453-491.

9. Vyshlov, A.S., 1976. Preliminary results of circumlunar plasma research by the Luna 22 spacecraft. Space research xvi, pp.945-949.